Pure & Appl. Chem., Vol. 59, No. 12, pp. 1673–1680, 1987.
Printed in Great Britain.

INTERNATIONAL UNION OF PURE AND APPLIED CHEMISTRY

INORGANIC CHEMISTRY DIVISION

COMMISSION ON HIGH TEMPERATURE AND SOLID STATE CHEMISTRY*

CHARACTERIZATION OF Si_3N_4 POWDERS

Prepared for publication by

G. PETZOW[1] and R. SERSALE[2]

[1] Max-Planck-Institut für Metallforschung, Institut für Werkstoff-Wissenschaften, D–7000 Stuttgart 80, FRG

[2] Università degli Studi di Napoli, Istituto di Chimica Applicata, I–80125 Napoli, Italy

* Membership of the Commission during the preparation of this report (1983–87) was as follows:

Chairman: 1983–85 K. L. Komarek (Austria); 1985–87 R. Metselaar (Netherlands); *Secretary*: P. W. Gilles (USA); *Titular Members*: A–M. Anthony (France; 1983–85); J. F. Baumard (France; 1985–87); J. Corish (Ireland; 1985–87); L. V. Gurvich (USSR); R. Metselaar (Netherlands; 1983–85); G. Petzow (FRG; 1983–85); M. H. Rand (UK); *Associate Members*: C. B. Alcock (Canada; 1983–85); A–M. Anthony (France; 1985–87); J. B. Clark (Republic of South Africa; 1985–87); J. Corish (Ireland; 1983–85); J.–P. Coutures (France); J. Drowart (Belgium); E. Fitzer (FRG; 1983–85); L. N. Gorockhov (USSR; 1985–87); J. Hastie (USA); M. G. Hocking (UK); L. Kihlborg (Sweden); J. Matousek (Czechoslovakia; 1985–87); R. W. Ohse (FRG); G. M. Rosenblatt (USA; 1985–87); R. Sersale (Italy; 1983–85); W. L. Worrell (USA; 1983–85); H. Yanagida (Japan); *National Representatives*: M. S. E. El-Sewefy (Arab Republic of Egypt); E. J. Baran (Argentina; 1984–87); E. R. McCartney (Australia; 1983–85); P. Ettmayer (Austria: 1986–87); D.–S. Yan (Chinese Chemical Society); J. Matousek (Czechoslovakia; 1983–85); E. Fitzer (FRG; 1986–87); J. F. Baumard (France; 1983–85); F. Solymosi (Hungary; 1985–87); A. P. B. Sinha (India; 1985–87); R. Vernerkar (India; 1983–85); G. De Maria (Italy); S. Somiya (Japan; 1985–87); M. Badri (Malaysia; 1983–85); B. B. Muhammad (Malaysia; 1985–87); J. B. Clark (Republic of South Africa; 1983–85); A. Magnéli (Sweden; 1983–85); G. Bayer (Switzerland); G. M. Rosenblatt (USA; 1983–85); W. L. Worrell (USA; 1985–87); M. M. Ristić (Yugoslavia).

Characterization of Si_3N_4 powders

Abstract - High technology ceramics based on Si_3N_4 are manufactured by sintering high pure and fine grained Si_3N_4 powders at high temperatures and pressures. Chemical composition, phase distribution and physical properties of the Si_3N_4 powder particles are characterized in respect to their sintering behaviour which determines the microstructure as well as the bulk properties of the sintered materials. Impurities, α/β ratio and crystallinity, size, shape and microstructure of primary and secondary particles are analyzed.

INTRODUCTION

Highly developed ceramic materials based on silicon nitride require extremely pure and well characterized starting powders. The starting powder determines the sintering behaviour and the subsequent microstructure formation. Hence, the resulting material properties depend to a large extent on the starting powders and their manufacturing technique. One can obtain a wide variety of strength versus temperature, creep and oxidation behaviour depending on the purity and phase composition of the starting Si_3N_4 powders. But also the type and amount of sintering additives, milling and mixing procedures and sintering parameters will affect the material properties of Si_3N_4-ceramics.

From the most important powder preparation techniques, such as

- nitridation of Si (1),
- carbothermal reduction of SiO_2 with subsequent nitridation (2),
- gas phase reaction of silanes with NH_3 (3) and
- pyrolysis of polysilanes (4),

Si_3N_4 powders with large differences with respect to crystallinity and α/β-Si_3N_4 ratio are obtained. Despite different specific surface areas, particle shapes and sizes, these powders always contain a characteristic amount of impurities mainly free Si, C and O, table 1. The oxygen content particularly has a strong influence on sintering, solid solution and glass formation in Si_3N_4-based ceramics.

The main metallic impurities present in the Si_3N_4 starting powders are W, Al, Ca, Mg, Fe, Na and K etc. Ca and Mg, in particular, are known to favour intergranular glass formation which deteriorates the material properties at high temperatures. Depending on the composition of the starting powders and the corresponding phase relations, polyphase Si_3N_4-materials may be produced.

POWDER CHARACTERIZATION

Chemical analysis

Si and N. The determination of the chemical composition becomes more difficult because of the heterogeneous distribution of the elements in the Si_3N_4 powder. The Si can appear as SiO_2, SiC, Si_2N_2O, Silicides such as $FeSi_2$, and as free Si. The total amount of Si can be determined by standard wet chemical analysis using absorption spectroscopic methods. However the phase distribution of Si can only be evaluated by quantitative phase analysis (XRD) which is restricted by the sensitivity depending on the scattering behaviour of the phases.

The total amount of N can be determined, for example, by dissolution of the Si_3N_4 in a mixture of hydrofluoric and hydrochloric acids and ammonia determination by titration (5) or inert gas fusion technique at 2700 °C (6).

Table 1. Characteristics of various Si_3N_4 powders in dependence of the production process.

Impurities (wt.%)	1	2	3	4	5	6	7
$Oxygen_{total}$	1.3	1.5	1.5	1.65	1.0	1.5	1
$Carbon_{total}$	0.41	0.16	0.22	0.06	-	-	0.1
ΣFe,Ca,Al	0.16	0.07	0.025	0.06	0.03	0.065	0.007
Specific Surface (m^2/g)	8.6	23	11.9	4.8	3.7	3.6	12
crystallinity	100	100	100	100	60	100	100
ß-Si_3N_4	4	3	0	7	5	6	10
	nitridation of Si			Carbothermal reduction of SiO_2 and nitridation	Gas phase reaction of $SiCl_4$+ NH_3	thermal decomposition of $Si(NH)_2$	

1,2: H.C. Starck, FRG; 3: Toray Ind., Japan; 4: Toshiba Corp., Japan; 5: GTE, USA; 6: Ube Ind. Ltd., Japan; 7: Toyo Soda Man. Co. Ltd, Japan.

Table 2. Scheme of the chemical analysis of Si_3N_4 powders.

ELEMENTS, PHASES	TECHNIQUE	ELEMENTS, PHASES	TECHNIQUE
α/ß-RATIO, GLASS CONTENT, IMPURITY PHASES	X-RAY ANALYSIS	O, C	INERT FUSION
		IMPURITY ELEMENTS	AAS, AES, MS, EDAX
Si, N, O	WET CHEMICAL ANALYSIS		
		Si-H, Si-O	IR-, RAMAN-SPECTROSCOPY
O	NEUTRON ACTIVATION		

O and C. Similarly to the distribution of Si, O and C are bound in different ways. O is mainly found as a thin SiO_2 surface layer on the Si_3N_4 grains. Smaller amounts of O appear in oxynitrides such as Si_2N_2O or O-containing Si_3N_4-solid solutions. Commercial submicron Si_3N_4-powders exhibit a total amount of 1-3 wt.% O, table 1. O can be determined by neutron activation analysis (7) or inert gas fusion technique at 2700°C (6). The neutron activation analysis has an error of ± 0.01 wt.% at 1-3 wt.% O. A certain amount of O is desirable to accelerate the sintering kinetics of Si_3N_4 powders (8).

The C-content derives from carbides, mainly SiC and WC, as well as organic C. The determination of total C-content can be done by measurement of the CO_2 conductivity after Wösthoff. A very low C-content is desired so that no C-O and C-N gaseous products will be formed during sintering (9).

Metallic impurities. The determination of metallic impurities such as Fe, Al, Ca, Mg, Ti, Li, W, Na, K, etc. can be carried out by standard spectroscopic techniques (AAS, AES, XRF). Usually, the sum of Fe+Ca+Al-content is used to characterize the metallic impurity content. Powders with the sum less than 0.1 wt.% are called "pure" starting powders.

However a high Ca-content should be avoided in particular because Ca is known to be enriched in the glassy grain boundary layer and thereby lowering the softening point of the glass (10).

Anionic impurities. Anionic impurities as F^- and Cl^- result mainly from the specific powder preparation and purification processes. Their determination can be done also by spectroscopic methods (EDX). Additionally vibration spectroscopy, such as IR and Raman, can help to evaluate Si-H, Si-O and Si-N bonding and to describe amorphous states in the Si_3N_4 powder (11-14).

Table 2 summarizes a scheme for the chemical analysis of the Si_3N_4 starting powders.

Phase analysis

α/β-ratio and crystalline impurity phases. In addition to the impurity phases of Si_2N_2O, SiO_2 (crystalline and amorphous), SiC and Si, the α/β- ratio strongly influences the sinterability and microstructure formation of Si_3N_4 bodies. The most suitable procedure for evaluating the α/β-ratio in Si_3N_4 powders appears to be X-ray analyis. A review of the relevant literature suggests that the following reflections will provide most reliable ratio determination (15,16)

(210) for β-Si_3N_4 phase and
(210) for α-Si_3N_4 phase.

The diffracted intensity of a pure phase is given by

$$J = \frac{K\,R}{2\,\mu} \tag{1}$$

where K is a constant and R is a parameter which depends on the diffraction angle θ, Miller indices (hkl) and the type of material

$$R = \frac{1}{V^2}\, m\ (LP)\ /F/^2. \tag{2}$$

V is the volume of the unit cell, F is the structure amplitude, m is the multiplicity, LP is the Lorenz-polarization factor and μ is the linear absorption coefficient.

The evaluation of the volumetric ratio can be carried out by means of the following equation (17)

$$\frac{J_{\beta(210)}}{J_{\alpha(210)}} = \frac{R_{\beta(210)}}{R_{\alpha(210)}} \times \frac{c_\beta}{c_\alpha}\ . \tag{3}$$

$J_{i(hkl)}$ are the peak heights to approximate the diffraction intensities and $R_{i(hkl)}$ can be calculated on the basis of the more reliable crystallographic data. c_i are the volume fractions of α- and β-Si_3N_4, respectively.

In order to minimize the errors attributable to the preferential orientation phenomena and to size distribution of the phases, it is suggested to use $J_{i(hkl)}$ values corrected by means of an arithmetic mean. This implies taking the arithmetic mean of the intensity of a specific (hkl) reflection based on as many recordings on different samples as possible. It is advisable to use the reflections (101), (200), (201), (102), (210) and (301) for α-Si_3N_4 and (110), (200), (101) and (201) for β-Si_3N_4. In particular the procedure to be used is as follows:

1.) Calculate the normalized intensities $Y_{i(hkl)}$:

$$Y_{i(hkl)} = \frac{J_{i(hkl)}}{R_{i(hkl)}}\ , \tag{4}$$

2.) Average the normalized intensities:

$$Y_{avg\ i(hkl)} = \frac{\sum_{i=n}^{n} Y_{i(hkl)}}{n}\ , \tag{5}$$

3.) Calculate the corrected intensities:

$$(J_{i(hkl)})_{corr} = Y_{avg\ i(hkl)} \times R_{i(hkl)}\,. \tag{6}$$

For further improvement of the procedure, it is suggested to make the x-ray diffraction analysis using a spinning specimen holder and a slow scanning rate.

Provided that the impurity phases exceed a certain amount in the Si_3N_4 matrix, their amount can be determined in a similar way by quantitative x-ray analysis. The approximate detection limits are for Si_2N_2O > 0.5%, SiO_2 (crystalline) >0.7%, SiC > 0.8% and Si > 0.1% (17). Smaller amounts of impurity phases can only be detected by high resolution TEM techniques, which are also useful to describe the distribution of these phases.

Amorphous Si_3N_4

The Si_3N_4 can be partially amorphous. In particular gas phase reacted Si_3N_4 powders can obtain a high amount of amorphous Si_3N_4 phase, table 1. The weight fractions in the powder of the amorphous and crystalline Si_3N_4 phases can be determined as follows (18). A calibration curve relating the crystallinity to a parameter X is obtained by mixing in different ratios of amorphous and 100 % crystallized Si_3N_4 and a constant amount of internal standard of Si

$$X = \frac{J_{\alpha(avg)} + J_{\beta(avg)}}{J_{Si(avg)}} \quad . \tag{7}$$

where $J_{(avg)}$ is the normalized peak height of α- and β-Si_3N_4 as already mentioned and of (111) and (220) of Si. The normalization factors of the various diffraction peaks have been determined (15). The crystallinity of the Si_3N_4 powder can then be determined from the X-values using the calibration curve.

Solid solution characterization

Substitutional solid solution formation in the β-Si_3N_4 crystal structure is reported to occur in the systems SiAlON (19-21), SiBeON (22) and in the quinary system SiAlBeON (23). Further solid solution formation was reported with Mg and Li (24) and Ga (25). The solid solution composition can be represented by

$$Si_{6-x-y}Me^{3+}_x Me^{2+}_y O_{x+2y} N_{8-y-2y},$$

where Si^{4+} is replaced by Me^{n+} and N^{3-} by O^{2-}. The solid solution has a constant cation/anion ratio of 3/4. The most important examples are the β-SiAlONs with $Si_{6-x}Al_xO_xN_{8-x}$ where $x \leq 4.2$.

By introduction of cations such as Li, Mg, Y and rare earth elements, solid solution formation in the α-Si_3N_4 structure can be stabilized (26,27) and represented by

$$Me_x(Si,Al)_{12}(O,N)_{16}$$

with $x \leq 2$. Figure 1 gives the planes of constant cation/anion ratio of 3/4 for solid solution formation in the α- and β-Si_3N_4 structures for the MeSiAlON systems. In the case of Me = Y for example, the composition becomes

$$Y_xSi_{12-(3x+y)}Al_{3x+y}O_yN_{16-y}.$$

The solid solution level can be determined by measuring the lattice constants and by comparing standard curves. As an example figure 2a and b represents the dependence of the lattice parameters of β-SiAlON and α-SiAlON on composition (28,29).

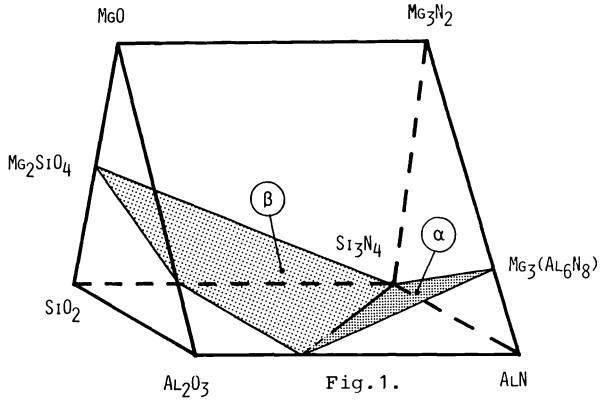

Fig.1. The system Al-Mg-Si-O-N with the two planes with constant cation/anion ratio where α- or β-Si_3N_4 solid solution can be formed.

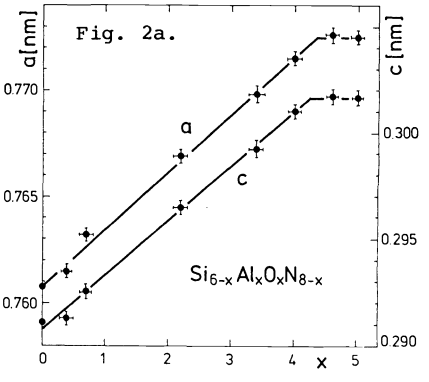

Fig. 2a. Dependence of the lattice parameters of β-$Si_{6-x}Al_xO_xN_{8-x}$ on the solid solution composition; after (28).

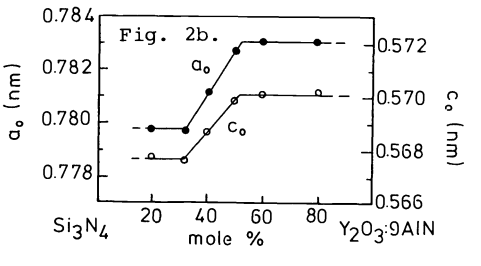

Fig. 2b. Lattice constants of yttrium-containing α-Si_3N_4 solid solution as a function of the composition; after (29).

Physical characterization

Crystallite and particle size. These two parameters are interrelated since a decrease in particle size or the anisotropic grain growth of Si_3N_4 particles will lead to an increase in specific surface. The importance of these factors arises from the influence they have on the basic operations of compacting and sintering. The α/β-transformation, solution-reprecipitation as well as diffusion processes are accelerated with decreasing particle size. However, very fine Si_3N_4 powders have certain disadvantages: they tend to have higher oxygen contents and poor flow properties, two factors which are of great importance when compacting and sintering Si_3N_4-powders.

One method by which the diameter (D) of the crystallites can be determined is from the x-ray line broadening (Δ). The method is based on Scherrer's equation:

$$D = \frac{S\ \lambda}{\Delta \cos \theta} \tag{8}$$

where λ is the radiation wave length and S a constant whose value depends upon the crystallite shape for the different diffraction orders (30). The broadening of the peak (Δ) is obtained after the comparison between the apparent width (Δ_A is the measured half-width of the peak) and the instrumental width (Δ_o), i.e. the peak width pertinent to crystals with dimensions greater than 1000 Å. So the peak broadening can be obtained by

$$\Delta = \sqrt{\Delta_A^2 - \Delta_o^2}\ . \tag{9}$$

For the crystallite size analysis by x-ray line broadening the α(301), α(222) and β(320) reflections are the most suitable.

Direct measurements of particle dimensions can be accomplished by TEM- observation.

While x-ray diffraction and TEM- observation only yield the size of the crystallites, other methods are required to describe the size of the primary particles, which are built up of agglomerated crystallites. The particles can then form agglomerates, which determine to a large extent the compaction and sintering characteristics of the Si_3N_4 powder. The agglomeration will be discussed later.

The size of the primary powder particles can be evaluated directly from SEM-micrographs or indirectly from the specific surface area (31). Sieving, sedimentation and permeability methods as for example FSSS (Fisher Sub Sieve Sizer) yield particle sizes that are shifted to higher values as compared to SEM-micrographs due to the influence of hard agglomerates. Deagglomeration procedures with surface active suspensions and ultrasonic waves therefore can strongly change the particle sizes and must be taken into account when these methods are applied to determine particle size.

Agglomeration and surface area

The formation of agglomerates tends to increase with decreasing particle size. In particular ultrafine Si_3N_4- powders require careful powder processing to avoid the formation of hard agglomerates, which can not be destroyed by ultrasonic waves and finally form defects during sintering. The tendency to form agglomerates can be described by direct observation of the agglomerates in a powder infiltrate in the SEM.

Also the ratio of the mean sizes of primary particles to deagglomerated particles is used to describe the agglomeration tendency of very fine Si_3N_4-powders (31).

The particle shape of the Si_3N_4 powders is of great importance. As mentioned earlier it significantly affects compacting properties. To characterize particle shape by means of a shape factor F_1 for convex particles (32)

$$F_1 = \frac{4\pi A}{U^2} \tag{10}$$

SEM or TEM micrographs can be evaluated using semi-automatic image analysis. A is the cross-sectional area and U the circumference of the Si_3N_4 grains in the micrographs. Isometric grains show F_1 to be about 1 with decreasing F_1 when elongated grain growth starts. Extended information on the relation of shape factors to surface and volume of the particles is given in ref. (33).

The surface area of a Si_3N_4 powder can be determined by an adsorption method, as typified by that of Brunauer, Emmett and Teller and known as the BET method. The use of this method has been well described in the literature (34).

Particle microstructure

Examination of particle microstructure i.e. intra-granular pores, nature of internal surfaces, surface stresses and powder defect structure follows well established techniques.

X-ray line broadening can be used to describe inhomogeneous internal stresses due to lattice distortions which can be introduced during mechanical powder treatment.

Based on the Bragg equation broadening of the lattice constants $\pm \Delta a/a$ is defined as

$$\frac{\Delta a}{a} = - \text{ctg } \theta \, \Delta\theta \qquad (11)$$

with θ being a high Bragg angle. Thus including the line broadening $\Delta(2\theta)_H$ at the half$_V$of the peak height internal stresses can be characterized by the parameter β_H as,

$$\beta_H^V = 4\frac{\Delta a}{a} \text{ tg } \theta_H . \qquad (12)$$

Dislocations, internal pores, interface and surface structure of the Si_3N_4 grains can only be examined by TEM or SEM techniques, respectively. Si_3N_4-powder samples for electron microscopy are prepared by evaporation of a Si_3N_4-suspension in water on a thin glassy foil or a copper grid. Subsequently the specimens are sputtered with gold under vacuum to avoid electrical charging.

Compaction characteristics

The compaction behaviour of Si_3N_4 powders determines to a large extent shaping and the properties of the green body. Good flow characteristics and homogeneous agglomerates are required to reduce defect formation in the green compact. The flow characteristics of fine grained Si_3N_4 powders is particularly influenced by agglomeration, their shape and size distribution. Spherical agglomerates of homogeneous size are wanted. For characterization of the flow behaviour the flow-meter can be used (35) as a standardized method. The density of the poured powder, that includes all pores between the Si_3N_4 particles, is measured as Scott density (36). In addition tap density canbbe determined, but this method can yield errors due to segregation in multicomponent powders with great differences in density as for example Si_3N_4 and Y_2O_3.

Shaping is particularly influenced by the pressing behaviour of the Si_3N_4 powder which is dependent on agglomeration, chemical composition, plasticity and the presence of surface films. Pressing under standardized conditions describes the pressing behaviour. After compaction the green density, which finally determines shrinkage, is to be evaluated geometrically or by weighting the sealed green compact in air and in water. The strength of the green compact (i.e. unsintered) may be determined in a variety of ways depending on the type of damage the part is likely to be exposed to during handling and transportation. One type of test is similar to the transverse rupture strength of the sintered material and the strength is measured by four point bending.

The methods used for characterization of the physical state of the Si_3N_4 powder are summarized in table 3.

Table 3. Physical characterization of Si_3N_4 powders.

PARAMETER	TECHNIQUE	PARAMETER	TECHNIQUE
CRYSTALLITE SIZE	X-RAY LINE BROADENING TEM-, SEM-POWDER MICROGRAPH	SPECIFIC SURFACE	GAS ABSORPTION (BET)
		PARTICLE MICRO-	X-RAY LINE BROADENING (HIGH ANGLE)
PARTICLE SIZE	SIEVING SEDIMENTATION TURBIDIMETRY	STRUCTURE	TEM, SEM MICROSCOPY PYCNOMETRY (HE)
	PERMEABILITY (FSSS)	COMPACTION CHA-	FLOW-METER
		RACTERISTICS	SCOTT DENSITY
AGGLOMERATION	SEM OF POWDER INFILTRATE		TAP DENSITY PRESSING
CRYSTALLITE AND PARTICLE SHAPE	SEM-, TEM-POWDER MICROGRAPH		TRANSVERSE RUPTURE STRENGTH

CONCLUSION

The increasing significance of Si_3N_4 as a high performance ceramic material with extremely good high temperature properties requires high purity starting powders having reproducible sintering properties. Because of the strong interdependence between the properties of the starting Si_3N_4 powder and the sintering behaviour, which determines the microstructure as well as properties of the sintered material an extensive characterization of the chemical and physical properties of the Si_3N_4-powder is demanded. Based on different production routes of the Si_3N_4 differences in the chemical and phase composition of the Si_3N_4 result so that the characterization procedures have to take into account the specific powder production process as well as the desired material properites.

Basically well developed methods for powder analysis are applicable but the extremely small grain size, high affinity to oxygen and variable phase composition are important features to be carefully taken into account. Due to the small grain size and impurity level high resolution detection techniques must be used, with various methods to be applied in combination. Further development of the sensitivity of physical techniques of analysis are desirable. This report can not attempt to deliver a complete and fixed instruction for the characterization of Si_3N_4 powders but it presents the present state-of-the-art of procedures that have proved to yield information which is important to characterize the behaviour of Si_3N_4 powders during sintering and the properties required for the particular application.

REFERENCES

1. D.R. Glasson, S.A.A. Jayaweera, J. Appl. Chem. 18, 65, (1968).
2. K. Komeya, H. Inoue, J. Mat. Sci., 10, 1244, (1975).
3. K.S. Mazdiyasni, C.M. Cooke, J. Am. Ceram. Soc., 56, 628, (1973).
4. S.K. Varshney, C.L. Beatty, Proc. 6th Ann. Conf. on Comp. and Adv. Ceram. Mat., Cocoa Beach, Florida, 555 (1982).
5. A. Parker and C. Healy, Analyst, 95, 204, (1970).
6. J. Mangels, J. Mat. Sci. Lett., 15, 2132, (1980).
7. W.R. Cannon, S.C. Danforth, J.H. Flint, J.S. Haggerty, R.A. Marra, J.Am. Ceram. Soc., 65, 324, (1982).
8. M. Mitomo, N. Kuramoto, Y. Inomata, J. Mat. Sci., 14, 2309, (1979).
9. H. Knoch, G.E. Gazza, J. Am. Ceram. Soc., 62, 634, (1979).
10. J.W. Edington, D.W. Rowcliffe, J.L. Henshall, Powd. Met. Int., 7, 82,
11. N. Wada, S.A. Solin, J. Wong, S. Prochazka, J. Non-Cryst. Solids, 43,(1981) 7.
12. S. Prochazka, C. Greskovich, Cer. Bull. 57 (1978) 579.
13. S. Wild, H. Elliott, D.P. Thompson, J. Mat. Sci. 13 (1978) 1769.
14. M. Hoch, T. Vernardakis, K.M. Nair, Sci.Cer. 10, 227, (1980).
15. C.P. Gazzara, D.R. Messier, Cer. Bull. 56, 777 (1977).
16. Z. Mencik, M.A. Short, C.R. Peters, in Advanc. in X-ray anal. 23, 375,(1980).
17. B. Krismer and G. Schwier, BMFT-Forschungsbericht 01-ZA 017-ZK/NT/NTS 1006, 1.8.1977-30.6.1980, Weiterführende Entwicklung und Herstellung von Siliciumnitrid-Alpha-Phase für das Heißpressen.
18. T. Yamada, T. Kawahito, T. Iwai, J. Mat. Sci. Lett. 2, 275, (1983).
19. K.H. Jack, W.J. Wilson, Nature, 238, 28 (1972).
20. Y. Oyama, O. Kamigaito, Jap. J. Appl. Phys. 10, 1637, (1971).
21. L.J. Gauckler, H.L. Lukas, G. Petzow, J. Am. Ceram. Soc., 58, 346, (1975).
22. I.C. Huseby, H.L. Lukas, G. Petzow, J. Am. Ceram. Soc., 58, 377, (1975).
23. L.J. Gauckler, H.L. Lukas, Mat. Res. Bull., 11, 503, (1976).
24. K.H. Jack, Trans. J. Brit. Ceram. Soc., 72, 376, (1973).
25. Y. Oyama, Jap. J. Appl. Phys., 12, 500, (1973).
26. S. Hampshire, H.H. Park, D.P. Thompson, K.H. Jack, Nature, 274, 880,(1978).
27. G. Grand, J. Demit, J. Ruste, J.P. Torre, J. Mat. Sci., 14, 1749, (1979).
28. L.J. Gauckler, J. Weiss, T.Y. Tien, G. Petzow, J. Am. Ceram. Soc., 61, 397, (1978).
29. Z.K. Huang, P. Greil, G. Petzow, Comm. Am. Ceram. Soc., 66, C-96, (1983).
30. G.P. Klug, E. Alexander, X-ray diffraction, ed. Alba, Torino, 492, (1969).
31. G. Schwier, Keramische Komponenten für Fahrzeug-Gasturbinen III, eds. W. Bunk, M. Böhmer and H. Kißler, Springer-Verlag, Berlin 55, (1984).
32. E.E. Underwood, Quantitative Stereology, Addison-Publ., Menlo Park, Calif., (1970).
33. T. Allen, Particle Size Measurements, Chapman and Hall Ltd., London, (1968).
34. B.C. Lippenca, M.A. Hermanns, Powd. Met., 7, 66, (1961).
35. C.G. Goetzel, Treatise on Powder Metallurgy, Interscience Publ. Inc., New York, 147, (1949).
36. ASTM-Standards, B 329, Part 7, (1967).